A Numerical Study of Bluff Ring Wake Stability

G.J. Sheard, M.C. Thompson and K. Hourigan

Department of Mechanical Engineering
Monash University, Clayton, Victoria, 3800 AUSTRALIA

Abstract

A numerical study of the wake dynamics and stability of the flow around bluff rings placed normal to the flow direction at low Reynolds number is presented. An attractive feature of this bluff body geometry is that it effectively behaves locally like a circular cylinder at high aspect ratio while, as the aspect ratio is reduced to zero, the body is transformed to a sphere. Thus, it covers a rich diversity of wake topologies and transitions. A spectral-element method is used to solve the unsteady axisymmetric Navier-Stokes equations governing the fluid flow. Wake stability is determined using a linear Floquet-type stability analysis. Strouhal-Reynolds number profiles are provided for a range of ring aspect ratios, as are critical Reynolds numbers for the onset of flow separation and periodic flow. A decrease in shedding frequency and an increase in the critical Reynolds numbers for separation and unsteady flow with decreasing ring aspect ratio is shown. Stability analysis has enabled interesting flow features with respect to the three-dimensionality of the flow to be obtained for different ring aspect ratios.

Introduction

Bluff body wake stability is an ongoing area of research, with many practical applications arising from knowledge of the dynamics of the wakes, and the transitions they undergo to turbulence. Much work has been carried out over the last century in the field of fluid dynamics on such geometries as spheres, cylinders, plates and discs, and these varied geometries provide some stark differences in their wake dynamics as well as other similarities. A ring of circular cross-section, d, and varied ring diameter, D, allows a wide scope of bluff geometries to be analysed in a simple two parameter space, with a Reynolds number, Re, governing the fluid, and an aspect ratio, $Ar = D/d$, governing the geometry. Hence an aspect ratio $Ar = 0$ denotes a sphere, and the limiting case as Ar tends to infinity is a straight cylinder. "Figure 1" shows a schematic diagram of the bluff ring system.
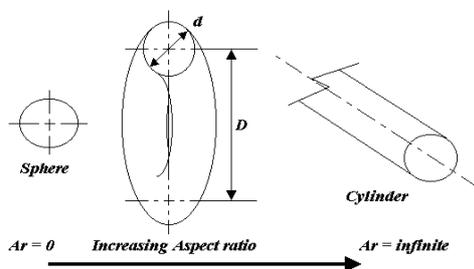

Figure 1. Schematic diagram of bluff ring system.

Large Ar rings have in fact been studied previously due to their similarities to the straight cylinder geometry, but without the resulting end effects associated with experimental work [3].

This paper contains descriptions of the numerical methods chosen to conduct the direct numerical simulations and stability analysis for this investigation. The grid resolution study is summarised with respect to the domain size of the final models generated.

Results of the 2D axisymmetric simulations are presented, with Strouhal profiles and critical Reynolds number profiles resulting from this work. Critical Reynolds numbers found are Re_1 (critical Reynolds number for flow separation from the ring cross-section), Re_2 (critical Reynolds number for wake unsteadiness), and Re_{3D} (critical Reynolds number for transition to 3D flow in the wake). The results of the stability analysis are presented in the form of Floquet multiplier profiles and profiles of the inferred critical Reynolds numbers for 3D flow. Finally plots of the streamwise vorticity of the perturbation field of the dominant modes for each ring is presented to gain insight into the nature of the likely 3D wakes.

Finally conclusions are drawn and acknowledgements made.

Numerical Formulation

The numerical simulations in this investigation were performed using a Spectral-Element method. This method is described in detail in [2] and [6]. Three-dimensional stability of the system was studied using the linear Floquet stability analysis technique.

Floquet stability analysis assesses the stability of a 3D perturbation superimposed over a 2D periodic base flow. [1] provides an excellent description of the technique as applied to the flow around a circular cylinder. The 3D perturbation is solved using linearised Navier-Stokes equations, and for simplicity only one spanwise mode number, β, is treated at a time. This corresponds to a spanwise wavelength of $\lambda = 2\pi/\beta$. In the axisymmetric formulation of the technique, this wavelength is expressed in radians, and only integer mode numbers satisfy the geometric limitations of the axisymmetric body. The implementation of the method in this case is somewhat different to [1], as the perturbation field is calculated in conjunction with the base flow, rather than as a post-processing step. The behaviour of the perturbation field is monitored throughout the simulation, and the result is expressed as a Floquet multiplier, μ, divulging the exponential behaviour of the perturbation. Multipliers $\mu > 1.0$ indicate a growing perturbation and hence an unstable base flow field. Conversely multipliers $\mu < 1.0$ represent a stable 2D flow. Thus a Floquet multiplier of $\mu = 1.0$ represents critical stability, where an applied perturbation neither grows nor decays.

Validation of Spectral-Element Method and Stability Analysis Technique

The Spectral-Element method used here is the same as that employed by [6], hence only validation of the meshes used in this investigation is required.

A thorough grid resolution study elucidated the sufficient compromise between computational efficiency and allowable accuracy in this investigation. For more information see [5].

The Floquet analysis technique was validated by comparing results obtained for straight cylinder and the sphere models with accepted values from experiment and numerical work.

Numerical stability analysis of the wake from flow around a sphere was carried out by [4]. They determined that the sphere wake becomes 3D at a Reynolds number of 210 (based on sphere diameter), undergoing a regular bifurcation and adopting a non-axisymmetric wake with a mode number $\beta = 1$.

Floquet analysis conducted on the steady 2D axisymmetric flow around a sphere was carried out over several Reynolds number to determine the critical point for a mode $\beta = 1$ instability of the wake. Linear interpolation between multipliers from simulations at $Re = 211$ and 212 give a critical Reynolds number for flow around the sphere as $Re_{3D} = 211.53 \pm 1.0$.

Similar studies were performed on the straight cylinder model. It is well known that two dominant 3D shedding modes exist for the straight cylinder. The first is "Mode A" shedding, which first occurs around $Re = 190$, and is periodic in the spanwise direction with a wavelength of about 4 diameters. The second "Mode B" instability has a spanwise wavelength of about $0.8d$, and occurs around $Re = 260$.

Results from [1] indicate that the critical Reynolds number for "Mode A" shedding is $Re = 188.5 \pm 1.0$ at a wavelength of 3.96 ± 0.02. Our investigations at seven wavelengths between 3.3 and 4.5 produced a critical Reynolds number of $Re = 185.8$. This value was found by linear interpolation, and is 1.4% below the value obtained in [1]. This can be explained by the slightly smaller transverse domain used in our meshes (25 units as opposed to 28 units). The spanwise wavelength at which this occurs is 3.936, obtained by polynomial interpolation. This value differs from the findings of [1] by just 0.6%.

These results validate the Floquet analysis technique employed, and show that dominant modes will be found with high accuracy, and the critical Reynold number values at which they arise will also be reasonably accurate.

Grid Resolution Study

A grid resolution study was carried out to determine sufficient domain size of the model to minimise blockage and boundary effects, while still maintaining reasonable computational efficiency. Attention was also paid to choosing the optimum number of nodes per element (N), and minimising the number of macro-elements incorporated in the meshes. An inlet length of 15 units was used. Transverse and downstream dimenstions were 25 units. $N = 64$ elements were used for the generation of base flow fields, and the Floquet analysis was carried out using $N = 81$ elements for improved resolution at $Re > 250$.

Axisymmetric Bluff Ring Flow

Simulations were carried out for each of the 6 bluff ring aspect ratios under investigation, as well as on a straight cylinder and an axisymmetric sphere model for validation purposes.

The Reynolds number range from 10 to 250 was investigated at increments of 10, with Strouhal numbers in the near wake being recorded at each case where unsteady flow fields became periodic. All simulations were performed until any transients had decayed, resulting in fully developed steady or periodic flow fields at various Reynolds numbers.

The resulting Strouhal-Reynolds number profiles compared well with [3], and are provided in [5]. The flow fields around lower aspect ratios at a given Reynolds number were found to shed at lower Strouhal numbers. This is in keeping with the findings of [3, 5], although [3] investigated only larger aspect ratio rings ($Ar > 10$).

The following sections discuss the determination of the critical Reynolds numbers for flow separation, and wake unsteadiness.

Separation of flow from ring cross-section

Flow separation was observed by monitoring the wake length at Reynolds numbers just following recirculating wake formation, and observing the stagnation points around the ring cross-section. Straight cylinder results were also obtained to verify with values in the literature, and the results matched up well. A graph of the critical Reynolds numbers found over aspect ratio and ring curvature is provided in "figure 2".
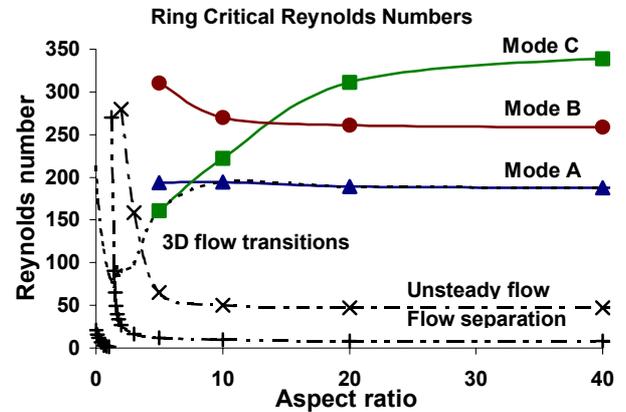

Figure 2. Critical Reynolds number profiles over bluff ring aspect ratio.

An interesting note is the rapid increase at lower aspect ratios of the critical Reynolds number for flow separation. This shows the poor representation of the model length scale at low aspect ratio by the ring cross-section diameter, d.

Observation of the velocity profiles at these low aspect ratios shows an interesting physical phenomenon. Rings of such low aspect ratio that no hole exists in the middle of the ring exhibit one large recirculation region behind them, similar to the sphere, which is present at Reynolds numbers of the same order as that for the recirculating wake behind a straight cylinder and the large rings. However at an aspect ratio larger than $Ar = 1$, where a hole is present in the middle of the ring, the large single recirculating wake disappears, being replaced by a recirculating bubble downstream of the ring. At higher Reynolds numbers, this bubble disappears, and flow separates from the ring cross-section.

The Onset of Unsteadiness in the Bluff Ring Wakes

The determination of the critical Reynolds number for the onset of unsteady flow in the ring wake was found by simply measuring the decay rate of unsteady velocity transients in the wake at a series of Reynolds numbers just prior to the onset of unsteady flow. Plotting of these values gave highly linear profiles that were extrapolated to the decay rate $k = 0$ to determine Re_2. "Figure 2" shows the trend of the critical Reynolds number for unsteadiness with aspect ratio. Note that as with the critical Reynolds number for flow separation, there is a sharp increase as aspect ratio is decreased. This is further support that the low aspect ratio ring flow behaviour is not well represented by a Reynolds number based on cross-section diameter, d.

No unsteady flow was achieved with the smaller aspect ratio 2D axisymmetric models; a result that was expected based on the propensity of the sphere wake to become unsteady only after a transition to a fully developed three-dimensional wake.

The remaining trends in "figure 2" pertain to the findings of the linear Floquet stability analysis applied to the 2D axisymmetric base flows already found. These will be discussed in the following sections.

Determining Ring 3D Stability Using Floquet analysis

A substantial amount of data was collected as part of a study of the stability of the bluff ring system to three-dimensional perturbations using the Floquet analysis technique discussed previously.

To begin the investigation, a study over many spanwise mode numbers was carried out for flow fields at a Reynolds number of 200, which is around the critical Reynolds numbers for three-dimensionality of the sphere ($Re \sim 211$) and the cylinder ($Re \sim 180$). It was hoped that the dominant modes in each case would reveal themselves as local maxima in the Floquet multiplier-Mode number profiles for each ring. Multipliers were also gathered for larger rings around the axisymmetric spanwise mode numbers treating a span length at the ring cross-section corresponding to the spanwise wavelengths of "Mode A" and "Mode B" shedding from previous straight cylinder Floquet analysis [1]. For large Ar rings, these mode numbers were sometimes very high. For example, "Mode B" for the $Ar = 40$ ring was expected to occur around a mode number of $\beta = 153$, or $0.82d$.

Multipliers were gathered at several Reynolds numbers around the dominant modes. Cubic and quadratic interpolations were used to better estimate the critical Reynolds number and spanwise wavelength of the transition. Critical Reynolds numbers found for secondary transitions should be treated with caution as the actual 3D flow field and the 2D base flow used for the stability calculations may differ. See [1] for a detailed description of the limitations of linear stability theory.

Modes of 3D shedding were observed in the unsteady flow fields associated with rings of aspect ratio $Ar \geq 5$. At smaller aspect ratios, the dominant Floquet modes occurred where the base flow was steady.

Dominant Spanwise Modes of 3D Instability

The graph in "figure 2" illustrates that 3D instabilities occur close to the critical Reynolds numbers for both "Mode A" and "Mode B" instabilities for the straight cylinder. The spanwise wavelengths at which these transitions were most unstable corresponded closely with the wavelengths for the "Mode A" and "Mode B" shedding modes respectively.
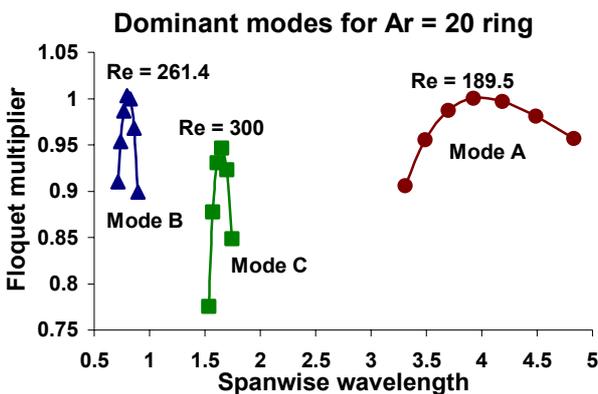
Dominant modes for Ar = 20 ring

Figure 3. Floquet multiplier profiles for the $Ar = 20$ ring. Note the Reynolds numbers for each local maximum, and the spanwise wavelength at which it occurs.

A third unstable mode was uncovered for various bluff rings. This mode had a spanwise wavelength between those of "Mode A" and "Mode B", around $1.6d$. The discovery of this intermediate wavelength mode, tentatively designated "Mode C" here, was unexpected.

Details of each mode will be investigated in the following sub-sections. As an illustration of the dominant mode behaviour for a bluff ring, "figure 3" is provided. The $Ar = 20$ ring is represented, and the three distinct modes can clearly be seen at their respective wavelengths.

"Mode A" Wavelengths for all Aspect Ratios

Around the spanwise wavelength at which "Mode A" shedding occurs for the straight cylinder, the bluff rings of all aspect ratios that exhibited periodic vortex shedding had a dominant Floquet mode that became critically unstable at Reynolds numbers between 185 and 200. These values are all close to the accepted value for the onset of "Mode A" 3D shedding in the straight cylinder wake. Observations of the streamwise vorticity of the perturbation field of these dominant Floquet modes for these wakes (see "figure 4") reveals a similarity to the findings of [1] relating to the straight cylinder. The perturbed wake maintained a similar single-period symmetry to the "Mode A" wake, and much of the streamwise vorticity is present within the vortex cores of the base flow vortex street. In each case the vorticity is concentrated in vortex cores close to the cross-section, but dissipates swiftly $8d$ to $10d$ downstream.
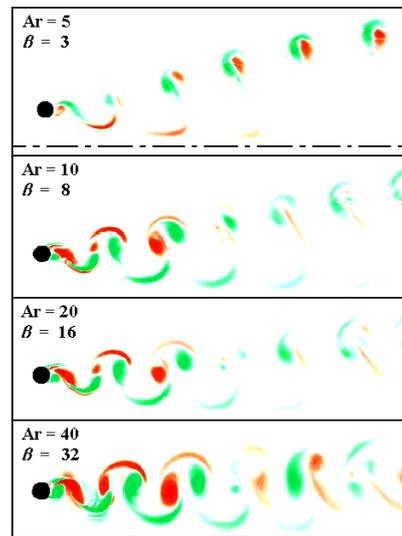

Figure 4. Streamwise vorticity of the perturbation field for the dominant mode associated with a "Mode A" spanwise wavelength for each ring. All simulations at $Re = 250$. Red indicates positive vorticity, and green is negative vorticity. Dashed line represents axis, ring cross-section represented by black circle, and flow is from left to right.

"Mode B" Wavelengths for Large Rings

As with the large-wavelength "Mode A" type instability, a small-wavelength "Mode B" type instability was also found for all shedding rings. The critical Reynolds number for this instability was as high as $Re = 310$ for $Ar = 5$, but approached the straight cylinder result of $Re = 258.4$ for the larger rings.

The Strouhal profiles found in experiment by Leweke & Provansal [7] are not discontinuous over the "Mode B" transition as the straight cylinder is. The gradient of the profile is discontinuous, however. In keeping with the present study, this discontinuity does occur at higher Reynolds numbers for smaller Ar rings.

The spanwise wavelength at which this mode was most unstable remains within 2% of the $0.812d$ found for the straight cylinder.

"Mode C" Wavelengths for all aspect Ratios

The intermediate-wavelength "Mode C" type instability occurs for all cases at about $1.6d$-$1.7d$. "Figure 2" shows that this instability occurs at higher Reynolds numbers as the ring aspect

ratio increases, but for lower aspect ratio rings it in fact becomes the dominant mode of spanwise instability. From "figure 2" it is obvious that somewhere between the $Ar = 5$ and $Ar = 10$ rings there exists a transition between "Mode A" dominant wakes, and wakes dominated by a "Mode C" shedding regime at lower aspect ratio from the crossing of the trends on the graph.
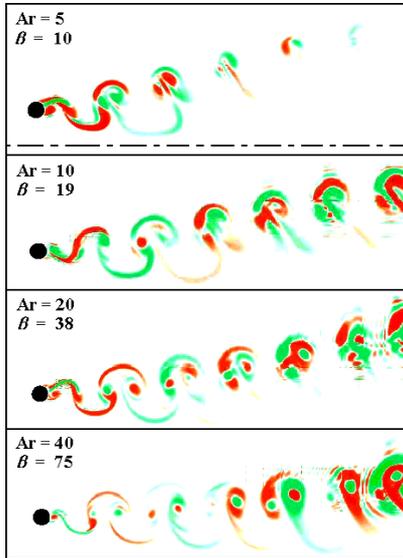

Figure 5. Streamwise vorticity of the perturbation field for the dominant mode associated with a "Mode C" spanwise wavelength for each ring. $Ar = 5$ at top to $Ar = 40$ at bottom. $Ar = 5$, $Ar = 10$ at $Re = 250$, $Ar = 20$ and $Ar = 40$ at $Re = 400$. Vorticity contours are between –0.5 and 0.5. Axis indicated as dashed line if shown.

The characteristics of the wake of a "Mode C" shedding regime can be inferred from the streamwise vorticity plots in "figure 5". Note that it is characterised by a two-period symmetry, and high vorticity in the braid regions between the vortex cores. Resolution in the far wake is poor in the larger ring wakes due to the higher Reynolds numbers of the simulations.

Instability of Steady Base Flows of Small aspect Ratio Rings

The Floquet analysis indicated that the $Ar = 2$ and $Ar = 3$ rings underwent a transition to three-dimensionality prior to a transition to unsteady flow of the 2D base flow. The dominant mode for the $Ar = 2$ ring was $\beta = 1$ as with the sphere, and for the $Ar = 3$ ring, the $\beta = 2$ spanwise mode dominates. This supports the hypothesis that the ring wake behaviour tends towards the sphere wake with decreasing aspect ratio.

The critical Reynolds number for the $Ar = 2$ ring was merely 90, adding further weight to the argument that low aspect ratio rings require a larger length scale to base their flow behaviour on than the ring cross-section diameter, d.

To compare with the perturbation fields for the shedding modes, streamwise vorticity plots have been provided for these dominant modes in "figure 6". The perturbation fields were obtained for $Re = 200$, and were in fact periodic. This indicated that a second transition had occurred in the wake from a 3D steady wake to a 3D shedding wake, similar to the second 3D instability for a sphere or disk investigated by [4]. The plots bear some resemblance to their findings, with slanted bands of alternating positive and negative vorticity convecting downstream of the body.
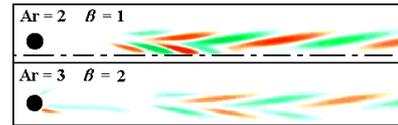

Figure 8. Streamwise vorticity of the perturbation field for the dominant mode of the $Ar = 2$ (top) and $Ar = 3$ (bottom) rings, both of which had a steady base flow. Flow calculated at $Re = 200$. The axis lies along the bottom of each frame, and contours are as per "figure 4".

Conclusions

We have presented results of both 2D axisymmetric direct numerical simulations, and Floquet linear stability analysis on the resulting base flows for the bluff ring system. Strouhal profiles and critical Reynolds number profiles have been presented, pertaining to the transitions to flow separation, unsteady flow, and likely three-dimensionality in the wake.

Floquet analysis has allowed us to make further predictions with respect to the three-dimensional wake structures based on the perturbation fields obtained, and comparison with existing work. Rings of $Ar = 2$ and $Ar = 3$ have been shown to undergo a transition to 3D flow prior to a transition to unsteady flow. Rings in the intermediate range around $Ar = 5$ appear to undergo a short spanwise wavelength 3D transition. Larger rings of $Ar = 10$ and greater have been shown to undergo an initial transition to 3D flow of a similar type to the "Mode A" shedding associated with straight cylinder flow.

Further investigation into rings of aspect ratio in the range $0 < Ar < 2$ is required to gain more thorough knowledge into the behaviour of the system. The task of carrying out exhaustive 3D numerical simulations to visualise the 3D wakes that may arise is the subject of continuing research at present.

References

[1] Barkley, *D.*, Henderson, R. *D.*, "Three-dimensional Floquet stability analysis of the wave of a circular cylinder", *J. Fluid Mech.*, **322**, 215-241, 1996.

[2] Karniadakis, G.E., "Spectral Element - Fourier methods for incompressible turbulent flows", *Comp. Methods in Appl. Mech. and Eng.*, **80**, 367-380, 1990.

[3] Leweke, T., Provansal, M., "The flow behind rings: bluff body wakes without end effects", *J. Fluid Mech.*, **288**, 265-310, 1995.

[4] Natarajan, R., Acrivos, A., "The instability of the steady flow past spheres and disks", *J. Fluid Mech.*, **254**, 323-344, 1993.

[5] Sheard, G., Thompson, M.C., Hourigan, K., "A 2D numerical study of the flow around bluff rings", *Melbourne Graduate Fluids Conference*, 2001

[6] Thompson, M.C., Hourigan, K., Sheridan, J., "Three-dimensional instabilities in the wake of a circular cylinder", *Exp. Therm. Fluid Sci.*, **12**, 190-196, 1996.

[7] Williamson, C.H.K.,"Oblique and parallel mode of vortex shedding in the wake of a circular cylinder at low Reyonlds numbers", *J. Fluid Mech.*, **206**, 579-627, 1989.